

Pharmacophore Modeling of Nilotinib as an Inhibitor of ABC Drug Transporters and BCR-ABL Kinase Using a 3D-QSAR Approach

Suneet Shukla¹, Abdul Kouanda¹, Latoya Silverton¹, Tanaji T. Talele², Suresh V. Ambudkar^{1*}

¹Laboratory of Cell Biology, Center for Cancer Research, National Cancer Institute, NIH, Bethesda, MD 20892

²Department of Pharmaceutical Sciences, College of Pharmacy and Health Sciences, St. John's University, Queens, NY 11439

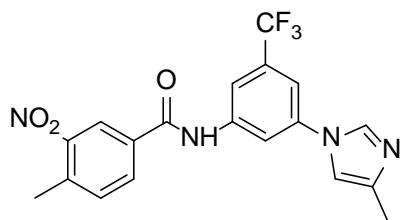
Supplementary Information (SI)

General experimental procedures.

Samples were analyzed for purity on an Agilent 1200 series LC/MS using a Zorbax Eclipse XBD-C8 reverse phase (5 micron, 4.6 x 150mm) column and a 1.1 mL/min flow rate. A gradient was performed using an acetonitrile/water mobile phase (each containing 0.1% trifluoroacetic acid). The gradient was 4% to 100% acetonitrile over 7 minutes. The purity of final compounds was determined to be >95%, using a two microliter injection with quantitation by AUC at 220 and 254 nanometers. High-res mass spectrometry was performed by the MSU Mass Spectrometry Facility and by the Analytical Chemistry group at the National Center for Advancing Translational Sciences, NIH. The ¹H spectra were recorded on a Varian Inova 400 MHz spectrometer. Chemical shifts are reported in ppm with the solvent resonance as the internal standard (DMSO-*d*₆: 2.50 ppm, MeOH-*d*₄: 3.31 ppm). Data are reported as follows: chemical shift, multiplicity (s = singlet, d = doublet, t = triplet, q = quartet, quin = quintet, sep = septet, br = broad, m = multiplet), coupling constants, and number of protons.

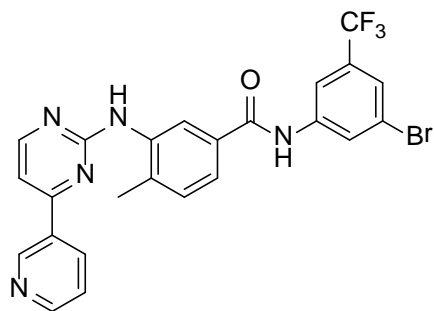
Synthesis of nilotinib and derivatives.

Nilotinib and its derivatives were synthesized by Drs. A.P. Skoumbourdis, D.Y. Duveau and C.J. Thomas (National Center for Advancing Translational Sciences, NIH, Rockville, MD 20850) using published methods as described previously.¹⁻³ The synthesis of nilotinib and its derivatives NCGC-2, NCGC-4, NCGC-15, NCGC-24, and NCGC-6 (referred as #1, #2, #3, #4 and #5 respectively, in³) has been described recently.³



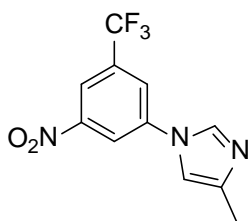
4-methyl-N-(3-(4-methyl-1H-imidazol-1-yl)-5-(trifluoromethyl)phenyl)-3-nitrobenzamide (NCGC-3)

¹H NMR (400 MHz, DMSO-*d*₆) δ 8.25 (d, *J* = 1.6 Hz, 1H), 7.81 (d, *J* = 2.0 Hz, 1H), 7.53 (t, *J* = 2.0 Hz, 1H), 7.47 (br. s, 1H), 7.43 (s, 1H), 7.35 (dd, *J* = 7.8, 2.0 Hz, 1H), 6.74 (s, 1H), 6.70 (d, *J* = 7.8 Hz, 2H), 1.85 (s, 3H), 1.60 (s, 3H); LC-MS: RT (min) = 4.53; [M + H]⁺ 405.1; HRMS calcd for C₁₉H₁₆F₃N₄O₃ (M + H) 405.1096, found 405.1171.



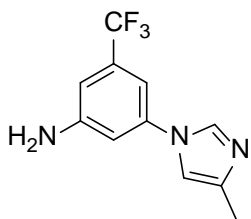
***N*-(3-bromo-5-(trifluoromethyl)phenyl)-4-methyl-3-(4-(pyridine-3-yl)pyrimidin-2-ylamino) benzamide (NCGC-5)**

^1H NMR (400 MHz, DMSO- d_6) δ 9.5 (s, 1H), 9.09 (d, J = 8.2 Hz, 1H), 8.86 (d, J = 5.1 Hz, 1H), 8.60 (d, J = 5.1 Hz, 1H), 8.42 (s, 1H), 8.27 (s, 1H), 8.10 (s, 1H), 8.01 (m, 1H), 7.72 (m, 1H), 7.57 (s, 1H), 7.51 (d, J = 5.1 Hz, 1H), 7.44 (d, J = 7.8 Hz, 1H), 2.42 (s, 3H); LC-MS: RT (min) = 5.73; $[\text{M} + \text{H}]^+$ 528.1; HRMS calc. for $\text{C}_{24}\text{H}_{18}\text{BrF}_3\text{N}_5\text{O}$ (M + H) 528.0569, found 528.0647.



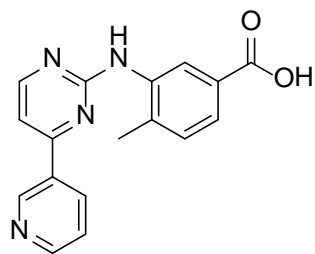
4-methyl-1-(3-nitro-5-(trifluoromethyl)phenyl)-1H-imidazole (NCGC-7)

^1H NMR (400 MHz, DMSO- d_6) δ 8.74 (t, J = 2.2 Hz, 1H), 8.51 (d, J = 1.2 Hz, 2H), 8.37 (m, 1H), 7.82 (t, J = 1.2 Hz, 1H), 2.17 (s, 3H); LC-MS: RT (min) = 3.64; $[\text{M} + \text{H}]^+$ 272.1; HRMS calcd for $\text{C}_{11}\text{H}_9\text{F}_3\text{N}_3\text{O}_2$ (M + H) 272.0569, found 272.0649.



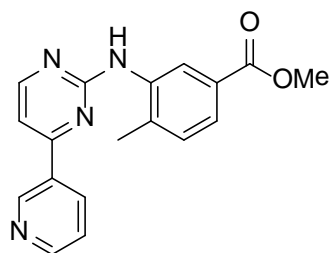
3-(4-methyl-1H-imidazol-1-yl)-5-(trifluoromethyl)aniline (NCGC-8)

^1H NMR (400 MHz, MeOH- d_4) δ 7.96 (d, J = 1.2 Hz, 1H), 7.23 (s, 1H), 6.93 (d, J = 1.6 Hz, 2H), 6.88 (s, 1H), 2.23 (s, 3H); LC-MS: RT (min) = 3.48; $[\text{M} + \text{H}]^+$ 242.1; HRMS calcd for $\text{C}_{11}\text{H}_{11}\text{F}_3\text{N}_3$ (M + H) 242.0827, found 242.0905.



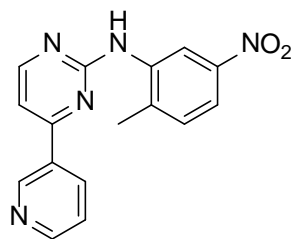
4-methyl-3-(4-(pyridine-3-yl)pyrimidin-2-ylamino)benzoic acid (NCGC-9)

^1H NMR (400 MHz, $\text{DMSO-}d_6$) δ 9.26 (d, $J = 1.6$ Hz, 1H), 9.01 (s, 1H), 8.68 (dd, $J = 4.7, 1.6$ Hz, 1H), 8.53 (d, $J = 5.1$ Hz, 1H), 8.44 (dt, $J = 8.1, 1.8$ Hz, 1H), 8.23 (s, 1H), 7.62 (dd, $J = 7.8, 1.6$ Hz, 1H), 7.52 (dd, $J = 7.6, 4.9$ Hz, 1H), 7.46 (d, $J = 5.5$ Hz, 1H), 7.30 (d, $J = 7.8$ Hz, 1H), 2.31 (s, 3H); LC-MS: RT (min) = 3.72; $[\text{M} + \text{H}]^+$ 307.1; HRMS calcd for $\text{C}_{17}\text{H}_{15}\text{N}_4\text{O}_2$ (M + H) 307.1117, found 307.1195.



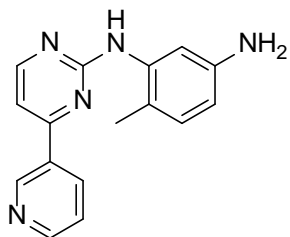
Methyl 4-methyl-3-(4-(pyridine-3-yl)pyrimidin-2-ylamino)benzoate (NCGC-10)

^1H NMR (400 MHz, CDCl_3) δ 9.29 (s, 1H), 9.03 (s, 1H), 8.68 (d, $J = 3.2$ Hz, 1H), 8.53 (d, $J = 4.8$ Hz, 1H), 8.42 (d, $J = 7.2$, 2H), 7.62 (d, $J = 7.6$, 1H), 7.51 (dd, $J = 4.8, 8.0$ Hz, 1H), 7.46 (d, $J = 5.2$, 1H), 7.35 (d, $J = 7.6$, 1H), 3.84 (s, 3H), 2.33 (s, 3H); LC-MS: RT (min) = 4.08; $[\text{M} + \text{H}]^+$ 321.1; HRMS calcd for $\text{C}_{18}\text{H}_{17}\text{N}_4\text{O}_2$ (M + H) 321.1273, found 321.1352.



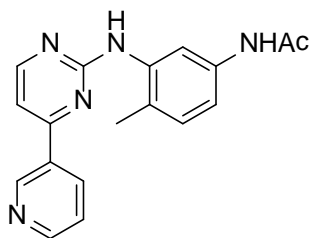
N-(2-methyl-5-nitrophenyl)-4-(pyridin-3-yl)pyrimidin-2-amine (NCGC-11)

^1H NMR (400 MHz, $\text{DMSO-}d_6$) δ 9.30 (s, 1H), 9.21 (s, 1H), 8.78 (s, 1H), 8.69 (d, $J = 4.0$ Hz, 1H), 8.32 (d, $J = 5.2$ Hz, 1H), 8.46 (d, $J = 8.0$ Hz, 1H), 7.88 (d, $J = 6.8$ Hz, 1H), 7.57-7.49 (m, 3H), 2.41 (s, 3H); LC-MS: RT (min) = 4.40; $[\text{M} + \text{H}]^+$ 308.1; HRMS calcd for $\text{C}_{16}\text{H}_{14}\text{N}_5\text{O}_2$ (M + H) 308.1069, found 308.1147



N-(2-methyl-5-aminophenyl)-4-(pyridin-3-yl)pyrimidin-2-amine (NCGC-12)

^1H NMR (400 MHz, $\text{MeOH-}d_4$) δ 9.20 (d, $J = 1.6$ Hz, 1H), 8.60 (dd, $J = 1.6, 5.2$ Hz, 1H), 8.47 (dt, $J = 8.0, 1.6$ Hz, 1H), 8.38 (d, $J = 5.2$ Hz, 1H), 7.52 (dd, $J = 8.0, 5.2$ Hz, 1H), 7.26 (d, $J = 5.6$, 1H), 7.1 (d, $J = 2.4$ Hz, 1H), 6.96 (d, $J = 8.4$ Hz, 1H), 6.51 (dd, $J = 8.0, 2.4$ Hz, 1H), 2.15 (s, 3H); LC-MS: RT (min) = 2.86; $[\text{M} + \text{H}]^+$ 278.1; HRMS calcd for $\text{C}_{16}\text{H}_{16}\text{N}_5$ (M + H) 278.1327, found 278.1406.

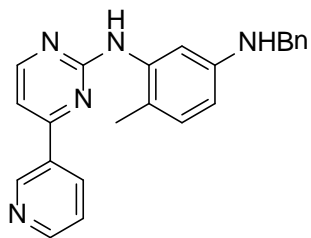


N-(2-methyl-5-acetylamino phenyl)-4-(pyridin-3-yl)pyrimidin-2-amine (NCGC-13)

^1H NMR (400 MHz, $\text{DMSO-}d_6$) δ 9.81 (s, 1H), 9.21 (d, $J = 1.6$ Hz, 1H), 8.87 (s, 1H), 8.64 (dd, $J = 4.8, 1.6$ Hz, 1H), 8.44 (d, $J = 5.2$ Hz, 1H), 8.39 (ddd, $J = 7.6, 2.4, 2.0$ Hz, 1H), 7.80 (d, $J = 2.0$ Hz, 1H), 7.48 (dd, $J = 8.0, 4.8$ Hz, 1H), 7.36 (d, $J = 5.2$ Hz, 1H), 7.23 (dd, $J = 8.0, 2.0$ Hz, 1H),

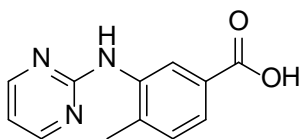
7.08 (d, $J = 8.4$ Hz, 1H), 2.13 (s, 3H), 1.98 (s, 3H); LC-MS: RT (min) = 3.50; $[M + H]^+$ 320.1;

HRMS calcd for $C_{16}H_{16}N_5$ ($M + H$) 320.3605, found 320.1511.



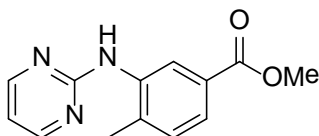
N-(2-methyl-5-benzylaminophenyl)-4-(pyridin-3-yl)pyrimidin-2-amine (NCGC-14)

1H NMR (400 MHz, $MeOH-d_4$) δ 9.22 (s, 1H), 8.61 (s, 1H), 8.45 (ddd, $J = 8.0, 2.0, 1.6$ Hz, 1H), 8.36 (d, $J = 5.2$ Hz, 1H), 7.52-7.48 (m, 2H), 7.34-7.14 (m, 5H), 7.04 (d, $J = 2.4$ Hz, 1H), 6.95 (d, $J = 8.4$ Hz, 1H), 6.43 (dd, $J = 8.4, 2.8$ Hz, 1H), 4.28 (s, 2H) 2.14 (s, 3H); LC-MS: RT (min) = 4.14; $[M + H]^+$ 368.1; HRMS calcd for $C_{23}H_{22}N_5$ ($M + H$) 368.1797, found 368.1877



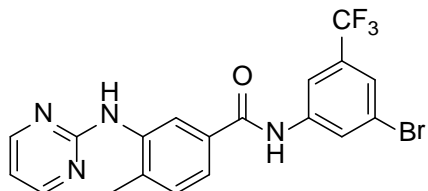
4-methyl-3-(pyrimidin-2-ylamino) benzoic acid (NCGC-16)

1H NMR (400 MHz, $DMSO-d_6$) δ 8.92 (s, 1H), 8.40 (s, 1H), 8.39 (s, 1H), 8.07 (d, $J = 1.6$ Hz, 1H), 7.62 (dd, $J = 7.8, 2.0$ Hz, 1H), 7.32 (d, $J = 7.8$ Hz, 1H), 6.79 (t, $J = 4.9$ Hz, 1H), 2.27 (s, 3H); LC-MS: RT (min) = 3.59; $[M + H]^+$ 230.1; HRMS calcd for $C_{12}H_{12}N_3O_2$ ($M + H$) 230.0851, found 230.0930.



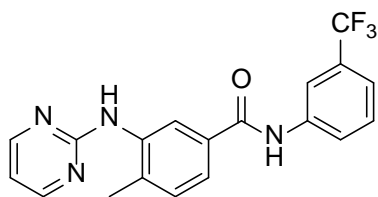
Methyl 4-methyl-3-(pyrimidin-2-ylamino)benzoate (NCGC-17)

^1H NMR (400 MHz, DMSO- d_6) δ 8.97 (s, 1H), 8.39 (d, $J = 4.8$ Hz, 1H), 8.05 (d, $J = 1.6$ Hz, 1H), 7.86 (d, $J = 1.6$ Hz, 1H), 7.68 (dd, $J = 7.6, 1.6$ Hz, 1H), 7.61 (dd, $J = 7.6, 1.6$ Hz, 1H), 7.35 (d, $J = 8.0$ Hz, 1H), 7.31 (d, $J = 8.0$ Hz, 1H), 6.78 (t, $J = 4.8$ Hz, 1H), 3.83 (s, 3H), 2.26 (s, 3H); LC-MS: RT (min) = 4.44; $[\text{M} + \text{H}]^+$ 244.1; HRMS calcd for $\text{C}_{13}\text{H}_{14}\text{N}_3\text{O}_2$ (M + H) 244.1008, found 244.1086.



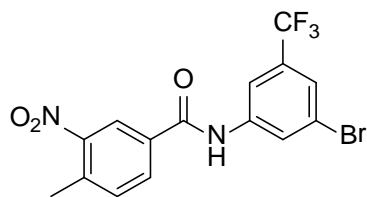
N-(3-bromo-5-(trifluoromethyl)phenyl)-4-methyl-3-(pyrimidin-2-ylamino)benzamide (NCGC-18)

^1H NMR (400 MHz, DMSO- d_6) δ 10.55 (s, 1H), 8.97 (s, 1H), 8.39 (d, $J = 4.8$ Hz, 2H), 8.37 (s, 1H), 8.23 (t, $J = 1.7$ Hz, 1H), 8.12 (d, $J = 1.8$ Hz, 1H), 7.71 (dd, $J = 7.9, 1.9$ Hz, 1H), 7.67 (s, 1H), 7.40 (d, $J = 8.0$ Hz, 1H), 6.79 (t, $J = 4.8$ Hz, 1H), 2.30 (s, 3H); LC-MS: RT (min) = 6.32; $[\text{M} + \text{H}]^+$ 453.0; HRMS calcd for $\text{C}_{19}\text{H}_{15}\text{BrF}_3\text{N}_4\text{O}$ (M + H) 451.0303, found 451.0381.



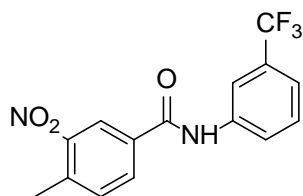
4-methyl-3-(pyrimidin-2-ylamino)-N-(3-(trifluoromethyl)phenyl)benzamide (NCGC-19)

^1H NMR (400 MHz, DMSO- d_6) δ 10.44 (s, 1H), 8.96 (s, 1H), 8.39 (d, $J = 4.8$ Hz, 2H), 8.28 – 8.09 (m, 1H), 8.06 (d, $J = 8.6$ Hz, 1H), 7.71 (dd, $J = 7.9, 1.9$ Hz, 1H), 7.59 (t, $J = 8.0$ Hz, 1H), 7.41 (dd, $J = 20, 7.9$ Hz, 2H), 6.78 (t, $J = 4.8$ Hz, 1H), 2.29 (s, 3H); LC-MS: RT (min) = 5.65; $[\text{M} + \text{H}]^+$ 373.1; HRMS calcd for $\text{C}_{19}\text{H}_{16}\text{F}_3\text{N}_4\text{O}$ (M + H) 373.1198, found 373.1276.



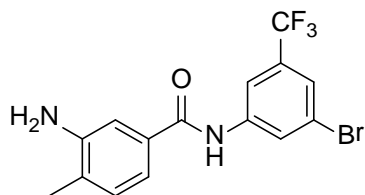
N-(3-bromo-5-(trifluoromethyl)phenyl)-4-methyl-3-nitrobenzamide (NCGC-20)

^1H NMR (400 MHz, DMSO- d_6) δ 10.84 (s, 1H), 8.61 (d, $J = 1.9$ Hz, 1H), 8.41 – 8.33 (m, 1H), 8.24 – 8.18 (m, 2H), 7.75 – 7.70 (m, 2H), 2.61 (s, 3H); LC-MS: RT (min) = 7.00; $[\text{M} + \text{H}]^+$ 405.0; HRMS calcd for $\text{C}_{15}\text{H}_{11}\text{BrF}_3\text{N}_2\text{O}_3$ (M + H) 402.9827, found 402.9897.



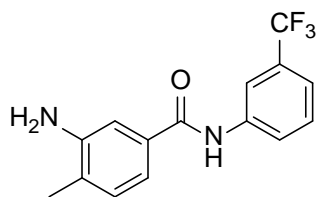
4-methyl-3-nitro-N-(3-trifluoromethyl)phenylbenzamide (NCGC-21)

^1H NMR (400 MHz, DMSO- d_6) δ 10.44 (s, 1H), 8.36 (d, $J = 1.9$ Hz, 1H), 8.21 (s, 1H), 7.64 (s, 1H), 7.19 (s, 1H), 7.16 – 7.05 (m, 3H), 2.13 (s, 3H); LC-MS: RT (min) = 6.39; $[\text{M} + \text{H}]^+$ 325.1; HRMS calcd for $\text{C}_{15}\text{H}_{12}\text{F}_3\text{N}_2\text{O}_3$ (M + H) 325.0722, found 325.0824.



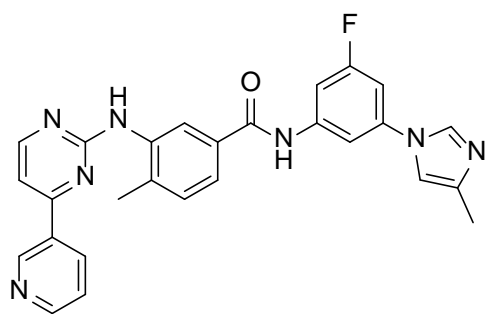
3-amino-N-(3-bromo-5-(trifluoromethyl)phenyl)-4-methylbenzamide (NCGC-22)

^1H NMR (400 MHz, DMSO- d_6) δ 10.44 (s, 1H), 8.36 (s, 1H), 8.21 (s, 1H), 7.64 (s, 1H), 7.19 (s, 1H), 7.17 – 7.01 (m, 2H), 5.26 (bs, 2H), 2.13 (s, 3H); LC-MS: RT (min) = 5.73; $[\text{M} + \text{H}]^+$ 375.0; HRMS calcd for $\text{C}_{15}\text{H}_{13}\text{BrF}_3\text{N}_2\text{O}$ (M + H) 373.0085, found 373.0162.



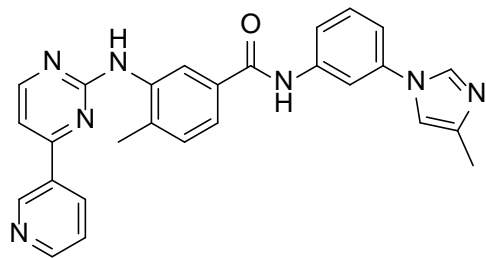
3-amino-4-methyl-N-(3-trifluoromethyl)phenyl)benzamide (NCGC-23)

^1H NMR (400 MHz, DMSO- d_6) δ 10.34 (s, 1H), 8.25 (bs, 1H), 8.05 (d, $J = 8.6$ Hz, 1H), 7.57 (t, $J = 7.8$ Hz, 1H), 7.41 (d, $J = 7.8$ Hz, 1H), 7.20 (d, $J = 1.6$ Hz, 1H), 7.12-7.05 (m, 2H), 5.10 (s, 2H), 2.12 (s, 3H); LC-MS: RT (min) = 4.97; $[\text{M} + \text{H}]^+$ 295.1; HRMS calcd for $\text{C}_{15}\text{H}_{14}\text{F}_3\text{N}_2\text{O}$ (M + H) 295.0980, found 295.1058



N-(3-fluoro-5-(4-methyl-1H-imidazol-1-yl)phenyl)-4-methyl-3-((4-(pyridin-3-yl)pyrimidin-2-yl)amino)benzamide (NCGC-25)

^1H NMR (400 MHz, DMSO- d_6) δ 10.69 (s, 1H), 9.52 (d, $J = 1.7$ Hz, 1H), 9.30 (d, $J = 2.2$ Hz, 1H), 9.19 (s, 1H), 8.72 (dd, $J = 4.8, 1.6$ Hz, 1H), 8.56 (d, $J = 5.2$ Hz, 1H), 8.51 (dt, $J = 8.0, 2.0$ Hz, 1H), 8.30 (d, $J = 1.9$ Hz, 1H), 8.12 (s, 1H), 7.95 (d, $J = 0.6$ Hz, 0H), 7.79 (dt, $J = 11, 2.1$ Hz, 1H), 7.75 (dd, $J = 8.1, 2.1$ Hz, 1H), 7.59 (dd, $J = 8.0, 4.8$ Hz, 1H), 7.50 (d, $J = 5.1$ Hz, 1H), 7.49 (dt, $J = 9.3, 2.2$ Hz, 1H), 7.45 (d, $J = 8.0$, 1H), 2.36 (s, 3H), 2.35 (s, 3H). LC-MS: RT (min) = 3.64; $[\text{M} + \text{H}]^+$ 480.1; HRMS calcd for $\text{C}_{27}\text{H}_{23}\text{FN}_7\text{O}$ (M + H), 479.1943; found, 480.1953.



4-methyl-N-(3-(4-methyl-1H-imidazol-1-yl)phenyl)-3-((4-(pyridin-3-yl)pyrimidin-2-yl)amino)benzamide (NCGC-26)

^1H NMR (400 MHz, DMSO- d_6) δ 10.54 (s, 1H), 9.53 (s, 1H), 9.28 (s, 1H), 9.17 (s, 1H), 8.70 (d, $J = 4.8$ Hz, 1H), 8.55 (d, $J = 5.1$ Hz, 1H), 8.48 (d, $J = 8.0$ Hz, 1H), 8.32 (t, $J = 2.1$ Hz, 1H), 8.29 (d, $J = 1.9$ Hz, 1H), 7.95 (s, 1H), 7.81 (d, $J = 8.4$ Hz, 1H), 7.75 (d, $J = 7.9$ Hz, 1H), 7.61 (t, $J = 8.1$ Hz, 1H), 7.58–7.52 (m, 1H), 7.49 (d, $J = 5.1$ Hz, 1H), 7.47 (m, 1H), 7.44 (d, $J = 8.4$ Hz, 1H), 2.36 (s, 3H), 2.36 (s, 3H). LC-MS: RT (min) = 3.52; $[\text{M} + \text{H}]^+$ 462.2; HRMS calcd for $\text{C}_{27}\text{H}_{24}\text{N}_7\text{O}$ (M + H) 462.2037; found, 462.2049.

References

1. Wei-Sheng, H.; William, C. S. An efficient synthesis of Nilotinib (AMN107). *Synthesis* **2007**, *14*, 2121-2124.
2. Duveau, D. Y.; Hu, X.; Walsh, M. J.; Shukla, S.; Skoumbourdis, A. P.; Boxer, M. B.; Ambudkar, S. V.; Shen, M.; Thomas, C. J. Synthesis and biological evaluation of analogues of the kinase inhibitor nilotinib as Abl and Kit inhibitors. *Bioorg. Med. Chem. Lett.* **2013**, *23*, 682-686.
3. Shukla, S.; Chufan, E. E.; Singh, S.; Skoumbourdis, A. P.; Kapoor, K.; Boxer, M. B.; Duveau, D. Y.; Thomas, C. J.; Talele, T. T.; Ambudkar, S. V. Elucidation of the structural basis

of interaction of the BCR-ABL kinase inhibitor, nilotinib (Tasigna) with the human ABC drug transporter P-glycoprotein. *Leukemia* **2014**. DOI 10.1038/leu.2014.21.

Table S1. Angles (°) between pharmacophore feature sites of P-gp, ABCG2 and BCR-ABL kinase inhibitors

P-gp, AADDRRR.990				ABCG2, ADHRRR.12				BCR-ABL, AADDRRR.2187			
Site1	Site2	Site3	Angle	Site1	Site2	Site3	Angle	Site1	Site2	Site3	Angle
A5	A1	D6	52.6	D7	A5	H8	67.8	A5	A1	D6	47.5
A5	A1	D7	28.5	D7	A5	R13	60.5	A5	A1	D7	7.1
A5	A1	R13	33.4	D7	A5	R14	54.6	A5	A1	R13	26.6
A5	A1	R14	32.9	D7	A5	R15	112.8	A5	A1	R14	11.7
A5	A1	R15	69.3	H8	A5	R13	7.3	A5	A1	R15	58.4
D6	A1	D7	57.4	H8	A5	R14	122.4	D6	A1	D7	41.0
D6	A1	R13	26.9	H8	A5	R15	48.4	D6	A1	R13	23.5
D6	A1	R14	80.5	R13	A5	R14	115.0	D6	A1	R14	59.0
D6	A1	R15	21.7	R13	A5	R15	55.4	D6	A1	R15	12.7
D7	A1	R13	30.5	R14	A5	R15	161.3	D7	A1	R13	19.5
D7	A1	R14	27.0	A5	D7	H8	83.9	D7	A1	R14	18.7
D7	A1	R15	78.8	A5	D7	R13	67.9	D7	A1	R15	52.3
R13	A1	R14	54.8	A5	D7	R14	77.0	R13	A1	R14	38.2
R13	A1	R15	48.4	A5	D7	R15	45.7	R13	A1	R15	35.9
R14	A1	R15	100.2	H8	D7	R13	16.0	R14	A1	R15	69.5
A1	A5	D6	74.7	H8	D7	R14	160.7	A1	A5	D6	75.4
A1	A5	D7	85.2	H8	D7	R15	41.4	A1	A5	D7	157.1
A1	A5	R13	83.3	R13	D7	R14	144.7	A1	A5	R13	96.5
A1	A5	R14	93.9	R13	D7	R15	27.1	A1	A5	R14	148.2
A1	A5	R15	48.7	R14	D7	R15	120.9	A1	A5	R15	46.1
D6	A5	D7	88.0	A5	H8	D7	28.3	D6	A5	D7	83.3
D6	A5	R13	29.1	A5	H8	R13	9.2	D6	A5	R13	27.8
D6	A5	R14	141.9	A5	H8	R14	21.5	D6	A5	R14	135.7
D6	A5	R15	29.4	A5	H8	R15	61.3	D6	A5	R15	30.1
D7	A5	R13	60.6	D7	H8	R13	19.1	D7	A5	R13	60.7
D7	A5	R14	54.5	D7	H8	R14	6.9	D7	A5	R14	54.4
D7	A5	R15	98.1	D7	H8	R15	87.7	D7	A5	R15	113.4
R13	A5	R14	115.0	R13	H8	R14	12.2	R13	A5	R14	115.0
R13	A5	R15	52.3	R13	H8	R15	70.1	R13	A5	R15	55.8
R14	A5	R15	138.1	R14	H8	R15	81.6	R14	A5	R15	161.5
A1	D6	A5	52.8	A5	R13	D7	51.6	A1	D6	A5	57.1

A1	D6	D7	55.7	A5	R13	H8	163.5	A1	D6	D7	85.4
A1	D6	R13	66.3	A5	R13	R14	34.2	A1	D6	R13	82.1
A1	D6	R14	50.7	A5	R13	R15	87.5	A1	D6	R14	74.5
A1	D6	R15	36.8	D7	R13	H8	144.9	A1	D6	R15	20.9
A5	D6	D7	28.0	D7	R13	R14	17.5	A5	D6	D7	28.5
A5	D6	R13	33.0	D7	R13	R15	134.7	A5	D6	R13	31.5
A5	D6	R14	15.3	H8	R13	R14	162.3	A5	D6	R14	17.5
A5	D6	R15	81.9	H8	R13	R15	76.7	A5	D6	R15	75.0
D7	D6	R13	10.6	R14	R13	R15	119.8	D7	D6	R13	16.8
D7	D6	R14	13.1	A5	R14	D7	48.5	D7	D6	R14	12.7
D7	D6	R15	92.1	A5	R14	H8	36.2	D7	D6	R15	103.5
R13	D6	R14	20.7	A5	R14	R13	30.7	R13	D6	R14	23.9
R13	D6	R15	102.7	A5	R14	R15	11.3	R13	D6	R15	102.5
R14	D6	R15	85.0	D7	R14	H8	12.4	R14	D6	R15	91.5
A1	D7	A5	66.3	D7	A5	H8	67.8	A1	D7	A5	15.8
A1	D7	D6	66.9	D7	A5	R13	60.5	A1	D7	D6	53.6
A1	D7	R13	76.9	D7	A5	R14	54.6	A1	D7	R13	52.0
A1	D7	R14	92.1	D7	A5	R15	112.8	A1	D7	R14	92.7
A1	D7	R15	42.1	H8	A5	R13	7.3	A1	D7	R15	31.2
A5	D7	D6	64.0	H8	A5	R14	122.4	A5	D7	D6	68.2
A5	D7	R13	67.8	H8	A5	R15	48.4	A5	D7	R13	67.7
A5	D7	R14	77.0	R13	A5	R14	115.0	A5	D7	R14	77.0
A5	D7	R15	57.4	R13	A5	R15	55.4	A5	D7	R15	45.2
D6	D7	R13	10.1	R14	A5	R15	161.3	D6	D7	R13	15.9
D6	D7	R14	140.4	A5	D7	H8	83.9	D6	D7	R14	142.5
D6	D7	R15	25.0	A5	D7	R13	67.9	D6	D7	R15	23.0
R13	D7	R14	144.6	A5	D7	R14	77.0	R13	D7	R14	144.7
R13	D7	R15	35.0	A5	D7	R15	45.7	R13	D7	R15	27.4
R14	D7	R15	123.6	H8	D7	R13	16.0	R14	D7	R15	120.4
A1	R13	A5	63.3					A1	R13	A5	56.9
A1	R13	D6	86.8					A1	R13	D6	74.4
A1	R13	D7	72.5					A1	R13	D7	108.5
A1	R13	R14	68.8					A1	R13	R14	91.1
A1	R13	R15	49.3					A1	R13	R15	36.8
A5	R13	D6	117.9					A5	R13	D6	120.7

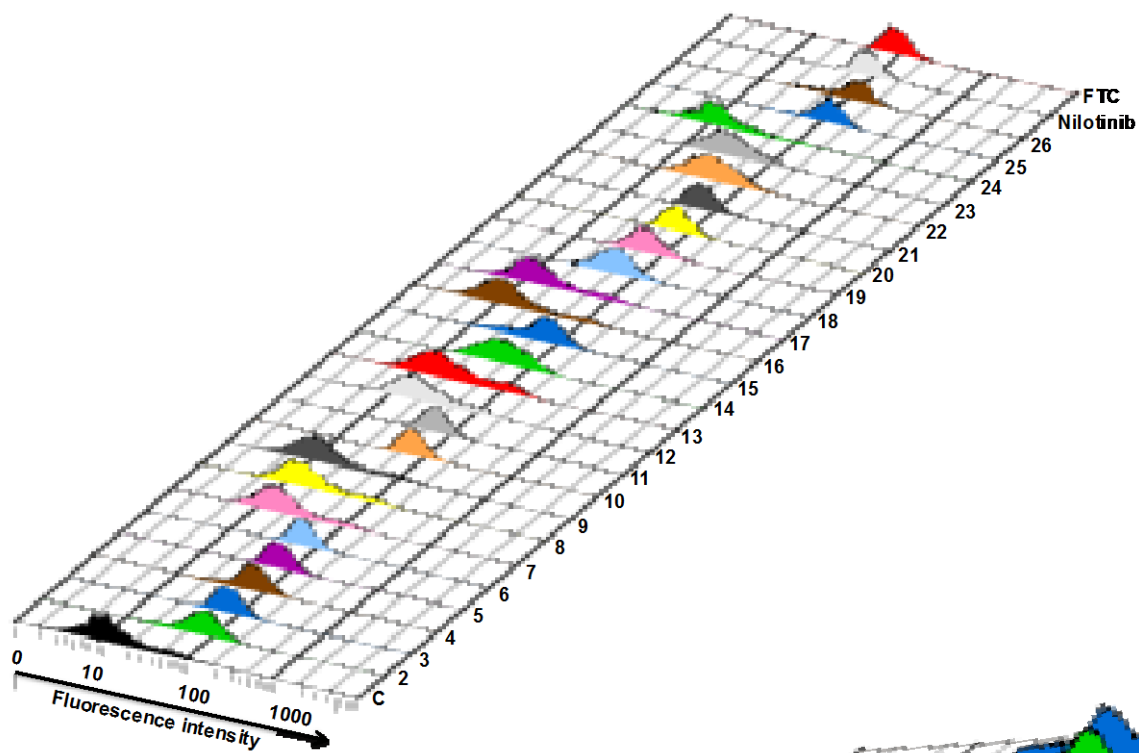
A5	R13	D7	51.6					A5	R13	D7	51.6
A5	R13	R14	34.2					A5	R13	R14	34.2
A5	R13	R15	92.2					A5	R13	R15	86.9
D6	R13	D7	159.3					D6	R13	D7	147.4
D6	R13	R14	149.1					D6	R13	R14	144.4
D6	R13	R15	37.7					D6	R13	R15	37.8
D7	R13	R14	17.5					D7	R13	R14	17.5
D7	R13	R15	121.6					D7	R13	R15	134.1
R14	R13	R15	114.4					R14	R13	R15	119.2
A1	R14	A5	53.3					A1	R14	A5	20.1
A1	R14	D6	48.9					A1	R14	D6	46.5
A1	R14	D7	60.9					A1	R14	D7	68.6
A1	R14	R13	56.4					A1	R14	R13	50.7
A1	R14	R15	31.0					A1	R14	R15	28.7
A5	R14	D6	22.8					A5	R14	D6	26.8
A5	R14	D7	48.5					A5	R14	D7	48.5
A5	R14	R13	30.7					A5	R14	R13	30.7
A5	R14	R15	25.8					A5	R14	R15	11.1
D6	R14	D7	26.5					D6	R14	D7	24.8
D6	R14	R13	10.2					D6	R14	R13	11.8
D6	R14	R15	18.8					D6	R14	R15	18.4
D7	R14	R13	17.9					D7	R14	R13	17.9
D7	R14	R15	39.6					D7	R14	R15	42.6
R13	R14	R15	28.0					R13	R14	R15	26.0
A1	R15	A5	62.0					A1	R15	A5	75.5
A1	R15	D6	121.5					A1	R15	D6	146.4
A1	R15	D7	59.1					A1	R15	D7	96.5
A1	R15	R13	82.2					A1	R15	R13	107.3
A1	R15	R14	48.8					A1	R15	R14	81.8
A5	R15	D6	68.7					A5	R15	D6	74.9
A5	R15	D7	24.5					A5	R15	D7	21.4
A5	R15	R13	35.5					A5	R15	R13	37.3
A5	R15	R14	16.1					A5	R15	R14	7.4
D6	R15	D7	62.9					D6	R15	D7	53.5
D6	R15	R13	39.6					D6	R15	R13	39.7

D6	R15	R14	76.2					D6	R15	R14	70.1
D7	R15	R13	23.3					D7	R15	R13	18.5
D7	R15	R14	16.8					D7	R15	R14	17.0
R13	R15	R14	37.6					R13	R15	R14	34.8

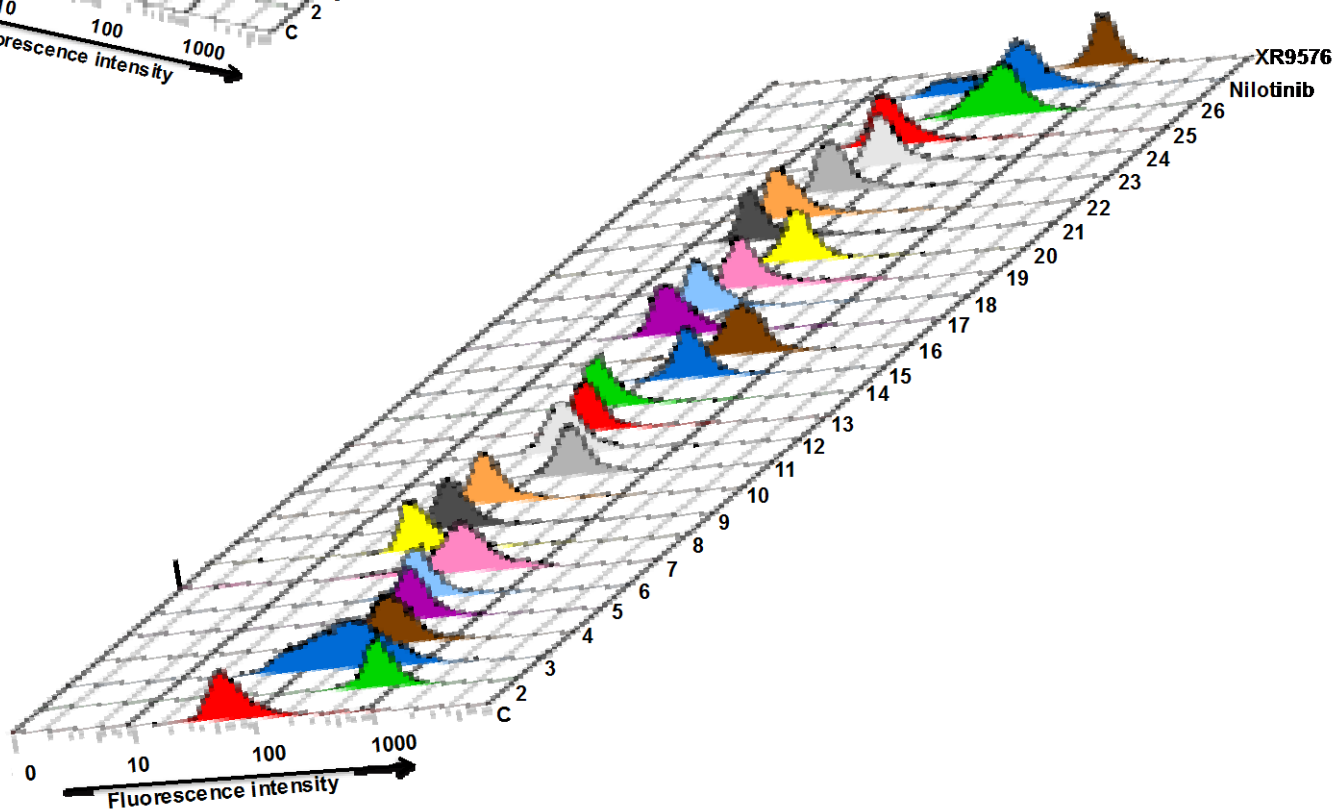
Supplementary Figure S1. Effect of nilotinib and its derivatives on ABCG2- or P-gp-mediated transport. Accumulation of mitoxantrone (ABCG2 substrate) (a, c) and calcein (generated from P-gp substrate calcein-AM) (b, d) was determined in the presence or absence of 10 μ M of nilotinib or indicated derivatives NCGC-2-NCGC-26 (marked as #2-#26) in ABCG2 and P-gp-expressing MCF7FLV1000 and KBV1 cells, respectively, as described in Experimental Section. 2 μ M Tariquidar (XR9576, a specific P-gp inhibitor) and 5 μ M FTC (a specific ABCG2 inhibitor) was used as a positive control to completely inhibit the activity of P-gp and ABCG2 respectively, in these assays. A representative histogram derived from CellQuest, which depicts the fluorescence intensity (log scale, X-axis) of mitoxantrone (a) and calcein (b), the cell number (Y-axis) and the indicated derivative (Z-axis) is shown here. The difference in the fluorescence intensity (accumulation levels) in the absence and presence of FTC or XR9576 (positive-control) inhibitors was taken as 100% activity and activity of the nilotinib or indicated derivative was calculated as % inhibitory activity compared to these controls. The graphs show % ABCG2 (c) or P-gp (d) inhibitory activity and error bars denote SD (n=3; Y-axis) in the presence of nilotinib, FTC, tariquidar or indicated derivative.

Supplementary Figure S1.

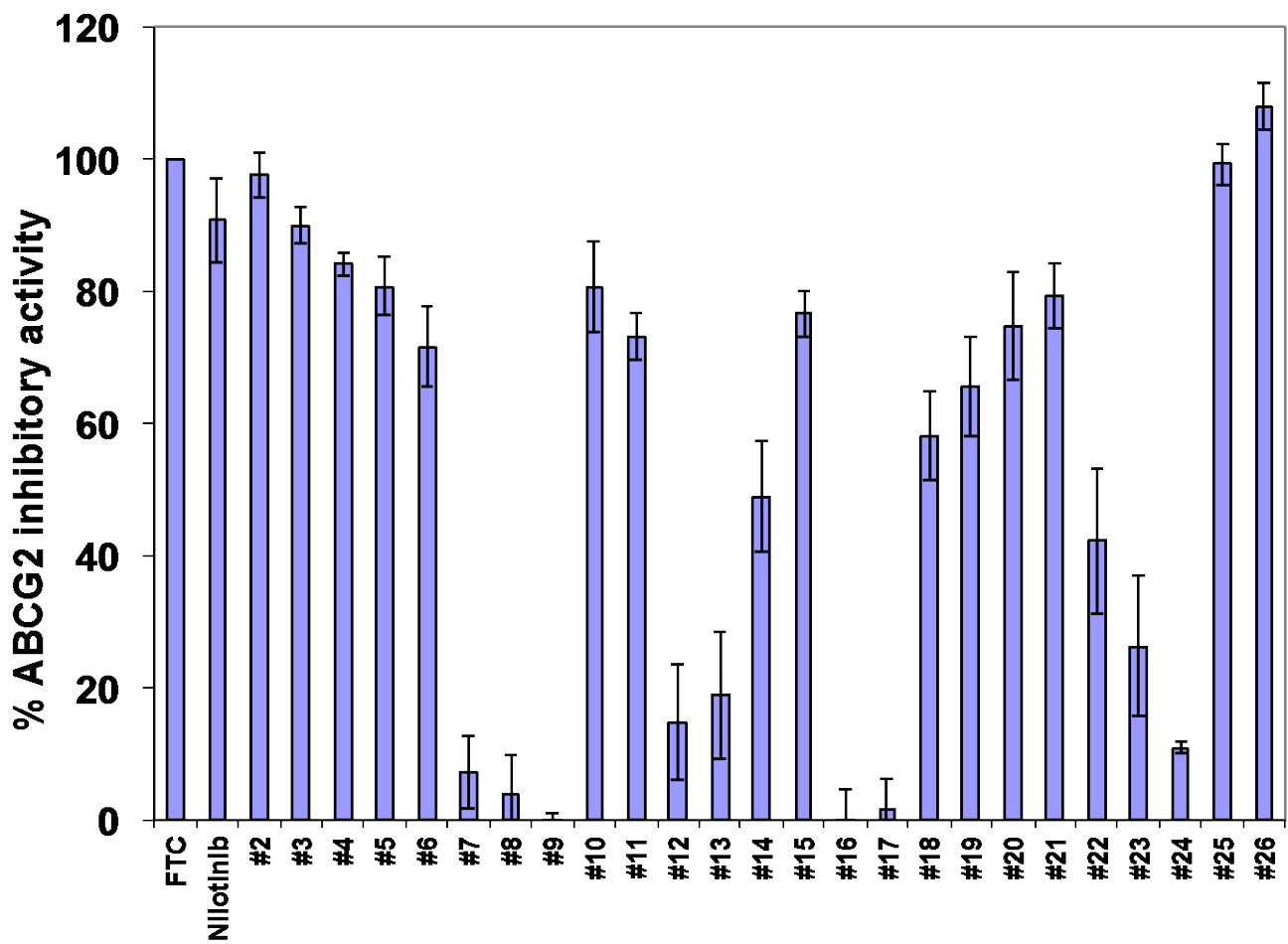
(a)



(b)



(c)



(d)

